Laboratory Investigation (2012) 92, 224–235

Antioxidant *N*-acetyl cysteine reverses cigarette smoke-induced myocardial infarction by inhibiting inflammation and oxidative stress in a rat model

Ashwani K Khanna[1,2], Jianping Xu[3] and Mandeep R Mehra[1,3]

The contribution of chronic tobacco exposure in determining post-myocardial infarction (MI) left ventricular (LV) remodeling and possible therapeutic strategies has not been investigated systematically. In this small animal investigation, we demonstrate that chronic tobacco smoke exposure leading up to acute MI in rats is associated with greater histological extent of myocardial necrosis and consequent worse LV function. These findings are associated with increased transcriptomic expression of pro-inflammatory cytokines, tissue repair molecules and markers of oxidative stress in the myocardium. The results demonstrate that an *N*-acetyl cysteine (NAC) treatment significantly reduced tobacco-exposed induced infarct size and percent fractional shortening. A significantly increased LV end-systolic diameter was observed in tobacco-exposed sham compared to tobacco-naïve sham (4.92 ± 0.41 *vs* 3.45 ± 0.33; $P < 0.05$), and tobacco-exposed MI compared to tobacco-naïve MI (8.24 ± 0.3 *vs* 6.1 ± 0.49; $P < 0.01$) rats. Decreased intracardiac mRNA expression of the markers of inflammation, tissue repair and oxidative stress and circulating levels of pro-inflammatory cytokines accompanied these positive effects of NAC. The treatment of tobacco-exposed MI rats with NAC resulted in significantly increased levels of intracardiac mRNA expression of antioxidants, including superoxide dismutase, thioredoxin and nuclear factor-E2-related factor 2, as well as circulating levels of glutathione (7 ± 0.12 *vs* 10 ± 0.18; $P \leqslant 0.001$), where the levels were almost identical to the tobacco-naïve sham rats. These findings identify a novel post-infarction therapy for amelioration of the adverse effects of tobacco exposure on the infracted myocardium and advocate the use of dietary supplement antioxidants for habitual smokers to prevent and reverse cardiovascular adverse effects in the absence of successful achievement of cessation of smoking.

Laboratory Investigation (2012) **92,** 224–235; doi:10.1038/labinvest.2011.146; published online 3 October 2011

KEYWORDS: antioxidants; cardiac dysfunction; cigarette smoke; myocardial infarction; Nrf2

Globally, tobacco smoke exposure remains a significant risk for the development of acute myocardial infarction (MI) irrespective of ethic or gender disparities. Exposure to tobacco smoke increases inflammation, oxidative stress[1–10] and decreases antioxidant expression.[11–15] Direct and indirect studies have demonstrated that oxidative stress from reactive oxygen species (ROS) generated through mitochondria, xanthine oxidase, and the NADPH oxidase system[16–21] is one of the important factors in the pathogenesis of myocardial ischemia. Decreased infarct size in superoxide dismutase (SOD)-producing transgenic mice suggests direct evidence for the role of involvement of ROS in MI.[22,23] In limited investigations, the use of antioxidants such as mercaptopropionyl glycine, edaravone and probucol have demonstrated varied effects on remodeling in animal models of MI,[24–32] with improvement in collagen content and histological changes. In this study, we sought to delineate the role of chronic tobacco smoke leading up to an acute MI by focusing on oxidative stress coupled with inflammation in the genesis of events leading to cardiac dysfunction and histological extent of damage. To further develop therapeutic targets, we tested the efficacy of *N*-acetyl cysteine (NAC), an antioxidant and anti-inflammatory agent in ameliorating the extent of myocardial damage and also investigated if facilitated repair could be augmented in a rat model of left anterior descending artery ligation-induced MI.

[1]Department of Pathology, University of Maryland, Baltimore, MD, USA; [2]OncoDetect, Baltimore, MD, USA and [3]Department of Cardiology, University of Maryland, Baltimore, MD, USA
Correspondence: Dr AK Khanna, PhD, Department of Pathology, University of Maryland, 19 Pine Street, MSTF Room 8-056, Baltimore, MD 21201, USA.
E-mail: akhanna@oncodetect.com

Received 21 April 2011; revised 22 July 2011; accepted 12 August 2011

MATERIALS AND METHODS

Exposure of Rats to Cigarette Smoke

This study was conducted according to the Guidelines for Animal Experiments of the NIH. Sprague–Dawley (SD) rats were exposed to cigarette smoke in a specially constructed smoke chamber.[1] The rats were restrained in the chambers and ventilated by the smoking machine. In this machine, smoke is sucked from lit cigarettes by syringes and pumped around the chamber. Rats that head to the smog compartment are additively inhaling the smoke from the tubing triggered from automatic controlled smoking generator. The smoking machine is set to inhale and exhale at intervals mimicking human smoking, with each cigarette lasting 8–10 min. Animals were under constant supervision to ensure that the animals were not distressed. The University of Maryland, Baltimore Animal Care and Use Committee approved all procedures. 3R4F research grade cigarettes with a regular amount of nicotine were used in this study (KTRDC Tobacco Biotechnology Group, University of Kentucky, Lexington, KY, USA). Animals were exposed to cigarette smoke 5 days per week for a total of 6 weeks with four cigarettes given intermittently throughout the day. Control rats were also kept in smoking chambers for four times a day, but without cigarette smoke equivalent to the time, the rats termed as tobacco naïve were exposed to cigarette smoke. The efficacy of cigarette smoke exposure was assessed by quantification of circulating levels of cotinine, the metabolite of nicotine using a kit from Calbiotech (Spring Valley, CA, USA).

The Rat Model of MI

Ligation of left descending artery

Model of MI in rats was created as described by us.[33] Before the induction of anesthesia, animals were examined to identify any pre-existing conditions that may complicate surgical outcome. Physical examination included visual inspection and measurement of heart rate, respiratory rate, body temperature and weight. MI was performed in SD rats based on sterilized microsurgery under general anesthesia on the water-circulating heating pad, which maintains the warm body temperature. First, the rats were atropinenized by the administration of atropine, intracerebrally (0.04 mg/kg), 15 min in advance of anesthesia. Then, the rats were anesthetized with ketamine/xylazine (100 mg/kg and 10 mg/kg) cocktail injected by peritoneum and followed by non-invasive ventilation (Harvard 683 rodent ventilator) with pure oxygen, and fixed on the surgical table covered by a sterile surgical drape. All instruments were autoclaved before first surgery and were sterilized with a hot bead sterilizer (Fine Science Tools 250 Hot Bead Sterilizer) for subsequent surgeries. The animal's left thorax was incised and the heart was exposed. LAD was confirmed and ligated with 7-0 polypropylene suture at 3 mm underneath the left atrium appendage. No sooner tighten ligation was made, and then infarction size and position were confirmed by visible blanching of the infarct area simultaneously and the elevated S–T segment in ECG to confirm the infarction. The chest was then closed. For *sham group*, the procedure is the same as above only with the intact LAD artery

Study design

MI in rats was created by ligation of left anterior descending artery and rats without ligation were used as sham; tobacco-naïve sham ($n=3$), tobacco-exposed sham ($n=3$), tobacco-naïve MI ($n=3$) and tobacco-exposed MI ($n=4$), tobacco-naïve MI plus NAC ($n=5$) and tobacco-exposed MI plus NAC ($n=5$) rats were used. Rats were exposed with four cigarettes per day for 6 weeks. Cardiac function was monitored by echocardiography, histological changes by Masson's trichrome staining (MTS) and molecular changes of pro-inflammatory cytokines, tissue repair molecules and markers of oxidative stress was studied by real-time PCR. All the studies were performed in animals killed after 6 weeks.

Treatment strategy

MI rats were treated with NAC (10 mg/kg per day), administered intraperitoneally, beginning the first day of surgery till 6 weeks. The treated animals ($n=5$, each MI group with or without tobacco exposure) were killed on week 6 after performing detailed echocardiography. Gross pathological analysis of the heart was performed; heart tissue, spleen and serum was saved at $-80\,^{\circ}C$ till analysis. All the experiments were performed blindly based on the ID of each animal.

Echocardiography analysis of sham and MI rats with and without exposure to cigarette smoke exposure

We performed echocardiogram-based morphological and functional assessment of all animals. After 30 days of cigarette smoke exposure, surgery was performed (sham or ligation of LAD). At 1 week after the surgery, transthoracic echocardiography (770 VisualSonics Ultrasound System, 17.5 MHz linear array transducer) was implemented under anesthesia induced by 5% isoflurane and maintained by 2% isoflurane in O_2 with activated charcoal absorption filters (VaporGuard). Short- and long-axis 2D M-mode and Doppler data were collected. All static and dynamic images were recorded. The Doppler analyze the LV input and output blood flow spectrum. In addition, all the animals were also scanned randomly 24 h in advance of MI procedure to obtain baseline imaging data. The image of the left ventricle cavity was obtained by positioning the cursor in the M-mode at the papillary muscles, below the mitral valve plane. The heart structures were measured in at least five consecutive heart cycles. Measurement parameters included LV end-diastolic and end-systolic diameter (LVEDD and LVESD) in short- and long axis, respectively, end-diastolic LV anterior wall thickness, posterior wall thickness and lateral wall thickness (only in short axis). Fractional shortening (FS) was calculated as $FS\ (\%) = (100) \cdot ((LVEDD - LVESD)/LVEDD)$.

Each measurement was repeated three times for statistical analysis to avoid intraobserver errors.

Detection of mRNA by real-time PCR

We performed real-time quantitative RT-PCR using a Bio-Rad iCycler system (Bio-Rad, Hercules, CA, USA) as described earlier.[1] RNAs were isolated from cardiac tissues using a kit from Promega (Madison, WI, USA) and reverse-transcribed into cDNAs by using a cDNA synthesis kit from Invitrogen (Carlsbad, CA, USA). The primer sequences for each gene are shown in Table 1. The mRNA level of each sample for each gene was normalized to that of the β-actin mRNA. Relative mRNA level was presented as 2((Ct/β-actin−Ct/gene of interest)).

Quantification of Circulating Levels of Cytokines

The Bio-Plex rat cytokine assay was used for simultaneous quantitation of pro-inflammatory cytokines: IL-1α, IL-1β, IL-2, IL-6, IFN-γ and TNF-α according to the recommended procedure. In brief, the premixed standards were reconstituted in 0.5 ml of sample diluent, generating a stock concentration of 10 000 pg/ml for each cytokine as described.[1] The standard stock was serially diluted in the same diluent to generate 8 points for the standard curve. Serum samples from rats were diluted 1:10. The assay was performed in a 96-well filtration plate supplied with the assay kit. Premixed beads (50 μl) coated with target capture antibodies were transferred to each well of the filter plate and washed twice with Bio-Plex wash buffer. Premixed standards or samples (50 μl) were added to each well containing washed beads. The plate was shaken for 30 s, and then incubated at room temperature for 30 min with low-speed shaking. After incubation and washing, premixed detection antibodies (50 μl) were added to each well. The incubation was terminated after shaking for 10 min at room temperature. After washing three times, the beads were resuspended in 125 μl of Bio-Plex assay buffer. Beads were read on the Bio-Plex suspension array system, and the data were analyzed using the Bio-Plex Manager™ software with 5PL curve fitting.

Tissue processing, assessment of infarction and fibrosis

Upon removal, part of hearts were immediately suspended in formalin-containing storage vials, a part of cardiac tissue was rapidly frozen in liquid nitrogen and then at −80°C until processing. Two 5-μm sections of the hearts, one near the base and one at mid-ventricle, were stained with hematoxylin and eosin and MTS to facilitate determination of the degree of infarction, myocardial fibrosis and collagen deposition. The rats were killed immediately after 6 weeks of postoperative echocardiography. Hearts were excised with heparin (30 µg/kg, intraperitoneally), weighed and the entire heart from base to apex was cut into 1-mm-thick slices along the short axial plane. The parts of middle capillary muscle were kept in 10% formalin. For histological staining, the slices were further sectioned into 4-μm slides to examine infarct size and its percentile by MTS. Briefly, heart sections were deparaffinized and treated with a gradient (100–70%) of alcohol, washed in distilled water and stained with Weigert's iron hematoxylin solution for 10 min and slides were washed. For the cytoplasm and muscle, the sections were then stained in Biebrich scarlet-acid fuchsin solution for 10–15 min, again washed with distilled water and treated with phosphomolybdic-phosphotungstic acid solution for 10–15 min, at this step, and for collagen staining, slides were transferred to aniline blue solution for 5–10 min and rinsed with water and 1% acetic acid. Slides were dehydrated with 95% alcohol and mounted with resinous mounting medium. The infarct area was measured on

Table 1 Primer sequences of genes for real-time PCR

Gene	Sense sequence	Antisense sequence
β-actin	5′-CCCAGCACAATGAAGATCAA-3′	5′-GATCCACACGGAGTACTTG-3′
IL-6	5′-TCAAGGGAAAAGAACCAGACA-3′	5′-GTTTCAAATCACTCACCCATAC-3′
TNF-α	5′-GGTCTGAGTACATCAACCTGGA-3′	5′-GTCTGTGCCCACATGTTCC-3′
IFN-γ	5′-CCACTATGGATCAGGGAAGG-3′	5′-TCACAATGATTCCACCCACA-3′
$p22^{phox}$	5′-GCCATTGCCAGTGTGATCTA-3′	5′-AATGGGAGTCCACTGCTCAC-3′
TGF-β	5′-CCTGCCCCTACATTTGGA-3′	5′-TGGTTGTAGAGGGCAAGGAC-3′
MMP-2	5′-GCACCACCGAGGATTATGAC-3′	5′-CACCCACAGTGGACATAGCA-3′
SDF-1	5′-GCGCTCTGCATCAGTGAC-3′	5′-GTTGAGGATTTTCAGATGTTTGAC-3′
SOD	5′-CTGGACAAACCTCAGCCCTA-3′	5′-TGATGGCTTCCAGCAACTC-3′
TXN	5′-TGCCGACCTTCCAGTTCTAT-3′	5′-GGCTTCGAGCTTTTCCTTGT-3′
Nrf2	5′-ATGGCCACACTTTTCTGGAC-3′	5′-AGATGTCAAGCGGGTCACTT-3′
Keap-1	5′-CAGCGTGCTCGGGAGTAT-3′	5′-GCAGTGTGACAGGTTGAAGAAC-3′
PARP	5′-CCAGCAGAAGGTCAAGAAGAC-3′	5′-ACCTCCATGCTGGCCTTT-3′

short axial section from the section of slice corresponding to the position of middle papillary muscle of LV. Infarct size was calculated using computer-based planimetry software (ImageJ, NIH). Infarction area percentage was defined as the infarcted area divided by whole LV muscular area.

Statistical analysis

Student's *t*-test was used to assess differences between the group means for FS, LVES, LVED dimensions, gene expression and cytokine levels. The analysis was performed using a statistical software program (GraphPad, San Diego, CA, USA). Results are expressed as the mean ± s.e.m. and two-tailed significance determined at the level of $P<0.05$.

RESULTS

Circulating Levels of Cotinine

The levels of cotinine, expressed as mean ± s.e.m. (ng/ml), were 77.2 ± 8.4 and 0.83 ± 0.13 in serum samples from SD rats exposed to cigarette smoke and air, respectively.

Effect of Chronic Tobacco Smoke Exposure on Extent of MI

Cardiac function by echocardiography

Typical M-mode images of parasternal short- and long-axis view at the middle of the papillary muscle level were as follows: in the sham group without exposure to cigarette smoke (Figure 1a) and when exposed to chronic cigarette smoke (Figure 1b). Figure 1a shows normal wall motion in contrast to the hypokinetic motion in Figure 1b. The wall motion in hearts with infarction as shown in Figures 1c and d demonstrates decreased ventricular function. (The Figures also show how the LVEDD and LVESD were measured). A significant difference in calculated FS (%) was seen in sham rats with and without chronic tobacco exposure, and those with MI and chronic tobacco exposure demonstrated the most decrease in ventricular function. Interestingly, the FS (%) was similar in sham with chronic tobacco smoke exposure (Figure 1b) and MI rats without exposure to cigarette smoke (Figure 1c). Comparison of FS (%) in

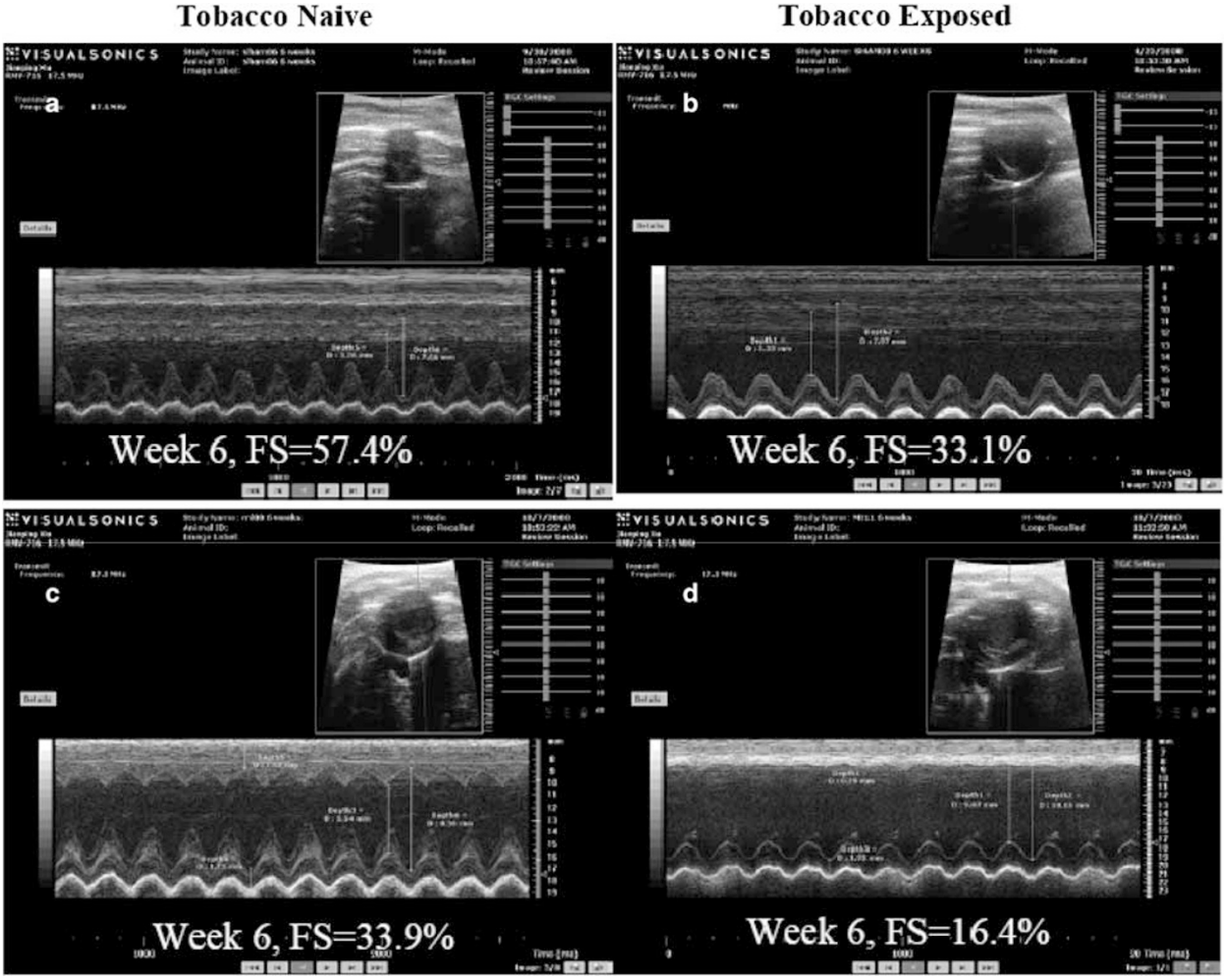

Figure 1 Typical M-mode images of parasternal short-axis view at the middle of the papillary muscle level: (**a**) representative tobacco-naïve sham group; (**b**) representative tobacco-exposed sham group; (**c**) representative tobacco-naïve myocardial infarction (MI) group; and (**d**) representative tobacco-exposed MI group. Calculated fractional shortening (%) is also shown for each animal.

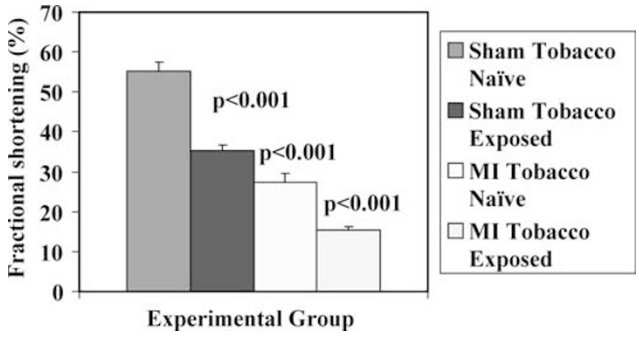

Figure 2 Effect of tobacco exposure on cardiac function: fractional shortening (%) in tobacco-naïve sham ($n=3$) and tobacco-exposed sham ($n=3$), and tobacco-naïve myocardial infarction (MI) ($n=3$) and tobacco-exposed MI ($n=4$) rats, expressed as mean ± s.e.m. Statistical analysis is represented as *P*-values for each group.

tobacco-naïve sham ($n=3$), tobacco-naïve MI ($n=3$), tobacco-exposed sham ($n=3$) and tobacco-exposed MI ($n=4$) rats is shown in Figure 2. A significantly decreased FS was observed in tobacco-exposed sham ($35.1 \pm 1.3\%$; $P<0.001$), tobacco-exposed MI ($15.4 \pm 0.2\%$; $P<0.001$) and tobacco-naïve MI ($27.4 \pm 2.3\%$; $P<0.001$) when compared to tobacco-naïve ($55.1 \pm 3.5\%$) rats.

Histological analysis of myocardium

Micrographs of Masson's trichrome-stained myocardial section are shown in Figure 3a. Short-axis MTS (magnification: $\times 10$) images from rats: sham (panel A) tobacco-naïve MI without (panel B) and with NAC treatment (panel C) and MI rats with chronic cigarette smoke without (panel D) and with (panel E) NAC treatment are shown. The tissue with blue staining is the infarcted area. The scar comprises dense collagen that signifies an infarct at the peri-infarction zone, and the collagen inter-digitates with viable myofibers.

Histopathological analysis at $\times 60$ is shown in Figure 3b. There was no significant fibrosis in tobacco-naïve sham, and development of fibrosis in tobacco-exposed sham was seen (blue stain in panel A). The photomicrographs of Masson's trichrome-stained heart sections in the infarct and peri-infarct regions from the tobacco-naïve MI rats group show comparatively less fibrosis (blue stain panel B) in the infarct and peri-infarct zone compared with tobacco-exposed MI (panel D), and marked attenuation of fibrosis in NAC-treated rats tobacco-naïve MI (panel C) and tobacco-exposed MI (panel E).

Quantification of infarct size is also shown in Figure 3c. Infract size in sham-operated rats was 0.6 ± 0.04 and significantly increased infarct size in cigarette smoke-exposed rats with MI was observed compared to tobacco-naïve rats (45.7 ± 2.1 *vs* 37.6 ± 0.56; $P=0.004$). NAC treatment of tobacco-exposed rats with MI resulted in a significant improvement in myocardial infarct size (45.7 ± 2.1 *vs* 25.4 ± 2.5; $P=0.0008$). Similarly, NAC treatment resulted in a significant decrease in infarct size (37.6 ± 0.56 *vs* 16.8 ± 0.86. $P=0.0001$) in tobacco-naïve rats. The results from each group of animals studied for weeks 1–6 are shown in Table 2.

Effect of the antioxidant NAC on tobacco smoke-related cardiac structure and function

Post-MI, rats were treated with NAC (10 mg/kg per day intraperitoneally) till 6 weeks. Echocardiography analysis was performed each week. A representative echocardiogram without and with NAC treatment is shown in Figures 4a and b. Compared to the first week, the FS (%) (15.4 ± 0.2) increased significantly ($P<0.001$) at 6 weeks (Figure 4b). A significantly increased LVESD compared to tobacco-naïve (3.45 ± 0.33) rats was observed in tobacco-exposed sham (4.92 ± 0.41; $P<0.05$), tobacco-exposed MI (8.24 ± 0.3; $P<0.01$) and tobacco-naïve MI (6.1 ± 0.49; $P<0.01$) rats. Treatment with NAC resulted in a significant decrease in LVESD (6.76 ± 0.48; $P<0.02$) compared to untreated group (8.24 ± 0.3). However, we did not observe any differences for LVEDD with or without either tobacco exposure or NAC treatment.

mRNA expression of inflammation, tissue repair and oxidative stress pathways and modulation by NAC

We demonstrate evidence of modulation of mRNA expression of inflammation, oxidative stress, tissue repair and antioxidant genes with and without NAC (Figures 5a, the mRNA expression was significantly higher in tobacco-exposed MI rats compared to tobacco-naïve MI rats for IL-6 ($P=0.001$) and TNF-α ($P=0.001$), IFN-γ ($P=0.001$) and $p22^{phox}$ ($P=0.001$)). Conversely, expression of SOD was significantly lower in tobacco-exposed MI rats compared to tobacco-naïve MI ($P=0.001$). However, there was no detectable thioredoxin (TXN) mRNA in either tobacco-exposed or -naïve MI rats. The expression of nuclear factor-E2-related factor 2 (Nrf2) mRNA increased significantly in tobacco-exposed MI compared to tobacco-naïve MI ($P=0.001$) rats; Kelch ECH-associating protein 1 (Keap-1) followed a similar trend ($P=0.05$) (Figure 5a). Similar results were obtained with mRNA expression of MMP-2 ($P=0.01$), stromal-derived factor-1 (SDF-1) ($P=0.01$), tumor growth factor (TGF)-β ($P=0.001$) and poly-(ADP-ribose) polymerase (PARP) that occurs in response to DNA damage ($P=0.001$) (Figure 5b). The mRNA expression for IL-6 ($P=0.001$), TNF-α ($P=0.001$), IFN-γ ($P=0.001$), $p22^{phox}$ ($P=0.001$), Nrf2 ($P=0.001$) and Keap-1 ($P=0.001$) in NAC-treated rats decreased significantly compared to tobacco-exposed MI rats (Figure 5b). Similar decrease in mRNA expression for MMP-2 ($P=0.001$), SDF-1 ($P=0.001$), TGF-β ($P=0.001$) and PARP ($P=0.001$) was observed in NAC-treated rats. In contrast, mRNA expression for antioxidants SOD ($P=0.001$) and TXN ($P=0.0001$) increased significantly in response to NAC.

Effect of NAC on circulating glutathione and pro-inflammatory cytokine levels

Glutathione levels: NAC is known to rapidly metabolize to intracellular glutathione, which acts as an antioxidant in the body. Therefore, we quantified serum levels of glutathione. There was a significant decrease in serum levels of glutathione in tobacco-exposed sham compared to tobacco-naïve sham rats (11.0 ± 0.37 *vs* 8.9 ± 0.7; $P = 0.04$), and

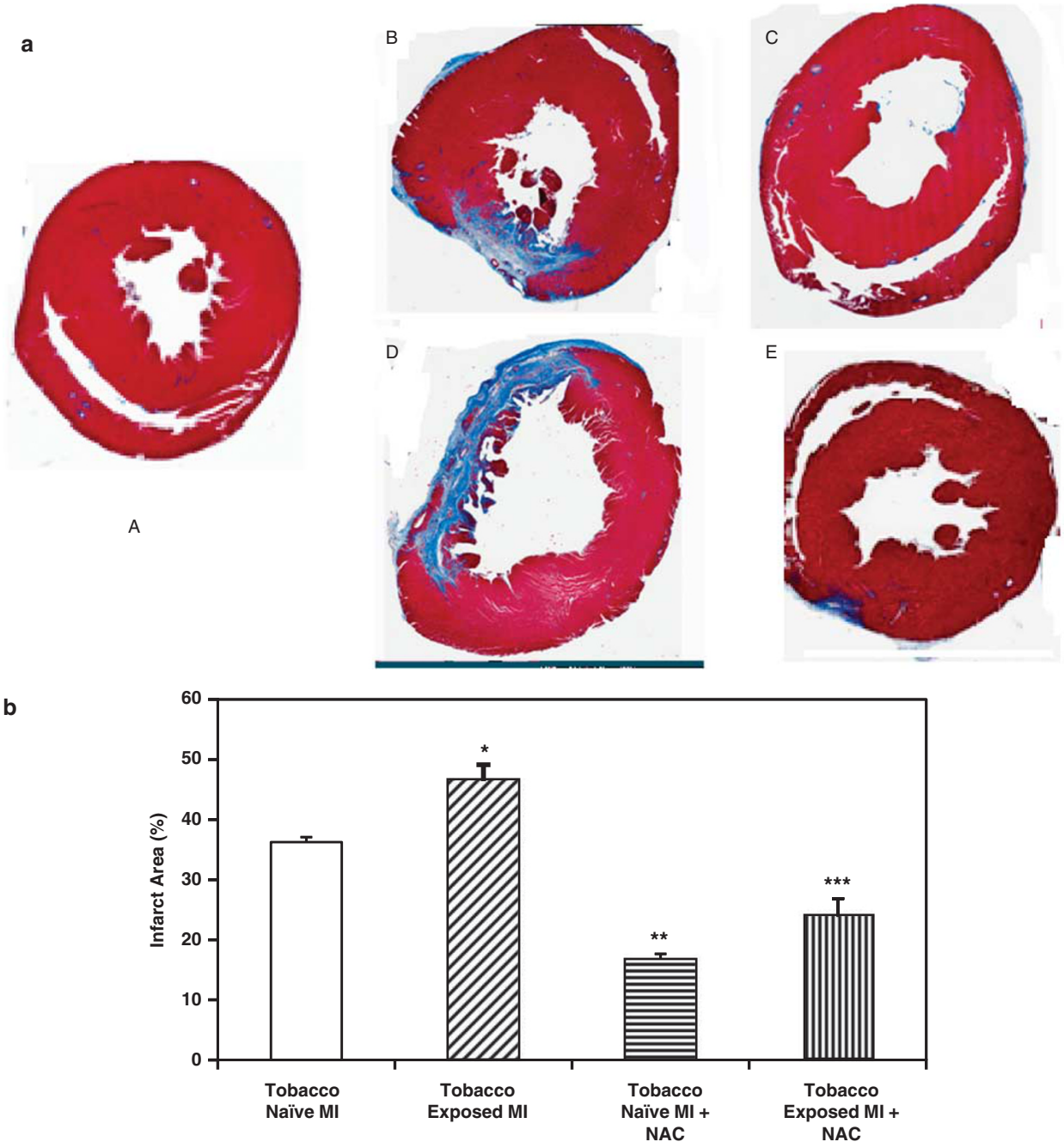

Figure 3 (**a**) Comparison of histology between the tobacco-naïve myocardial infarction (MI), tobacco-exposed MI and tobacco-exposed rats treated with *N*-acetyl cysteine: short-axis Masson's trichrome staining (MTS; magnification: $\times 10$) images; the tissue with blue staining is the infarcted area, which is shown for a representative rat from each group. (**b**) Comparison of histology at high power of magnification between the tobacco-naïve MI, tobacco-exposed MI and tobacco-exposed rats treated with *N*-acetyl cysteine: short-axis MTS (magnification: $\times 60$) images; the tissue with blue staining is the infarcted area, which is shown for a representative rat from each group; panel A, representative tobacco-naïve sham group; panel B, representative tobacco-exposed sham group; panel C, representative tobacco-naïve MI group; and panel D, representative tobacco-exposed MI group. (**c**) Mean ± s.e.m. of percent infarct size for each group is also shown. $^{*}P = 0.004$, $^{**}P = 0.0008$ and $^{***}P = 0.0001$.

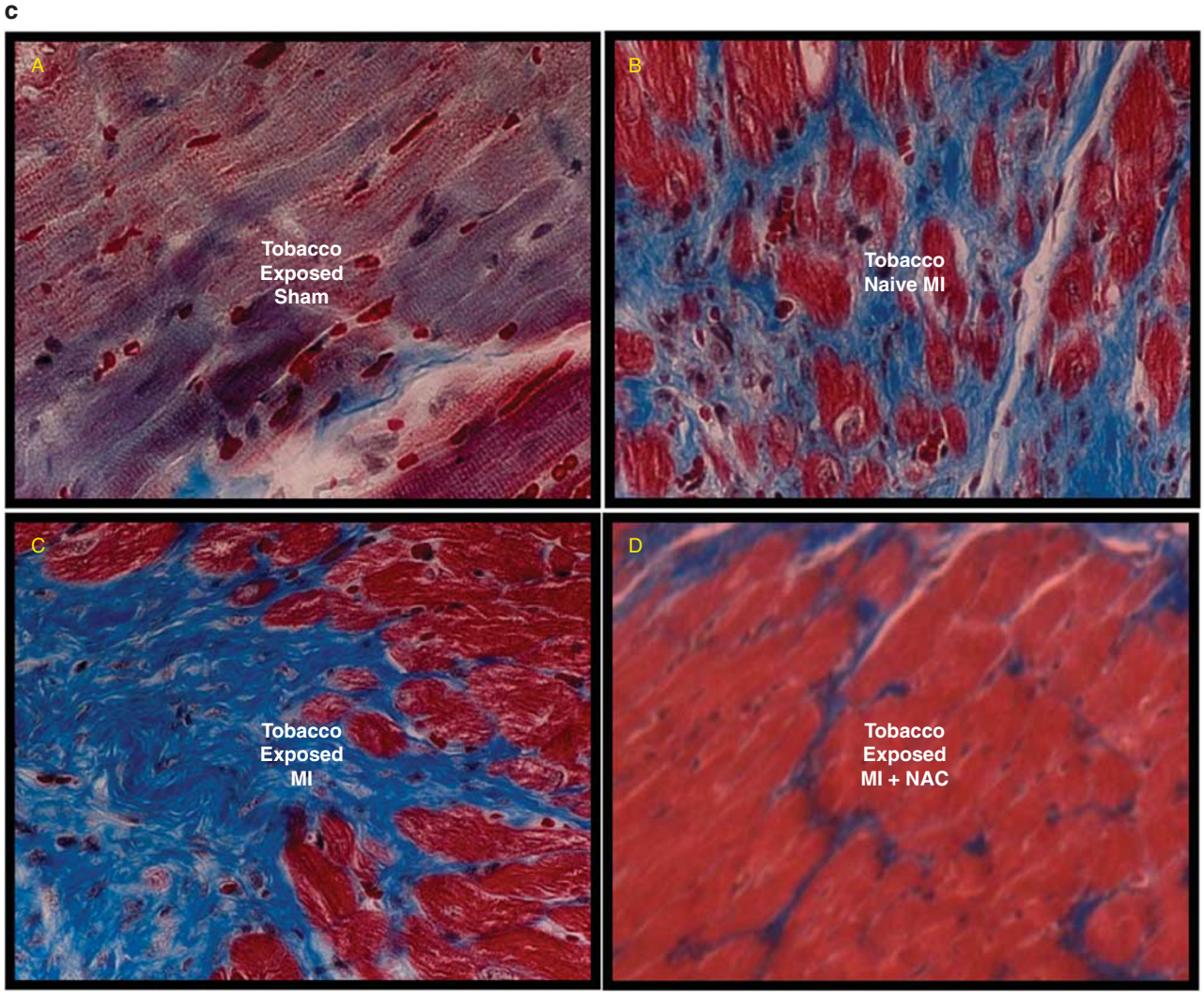

Figure 3 (Continued)

tobacco-exposed MI *vs* tobacco-naïve MI rats (8.0 ± 0.2 *vs* 7.0 ± 0.12; $P = 0.009$). However, treatment of tobacco-exposed MI rats with NAC resulted in significantly increased levels of glutathione (7 ± 0.12 *vs* 10 ± 0.18; $P = < 0.001$), the levels being almost identical to the tobacco-naïve sham rats (Figure 6).

Pro-inflammatory cytokine levels: We compared the circulating levels of cytokines IL-1α, IL-1β, IL-2, IL-6, IFN-γ and TNF-α in the sera obtained from sham-operated and MI rats with and without chronic exposure to tobacco (Figure 7). The circulating levels of IL-1α were significantly higher in tobacco-exposed sham compared to tobacco-naïve sham (963 ± 75 *vs* 243 ± 62; $P = 0.001$) and in tobacco-exposed MI compared to tobacco-naïve MI rats (1271 ± 143 *vs* 849 ± 88; $P = 0.05$). The circulating levels of IL-1β were significantly higher in tobacco-exposed sham compared to tobacco-naïve sham rats (2862 ± 28 *vs* 466 ± 16; $P = 0.001$) and in tobacco-exposed MI compared to tobacco-naïve MI rats (3014 ± 326 *vs* 1916 ± 110; $P = 0.01$); IL-2 levels were significantly higher in tobacco-exposed sham compared to tobacco-naïve sham rats (1278 ± 8 *vs* 24 ± 28; $P = 0.001$) and in tobacco-exposed MI compared to tobacco-naïve MI rats (1766 ± 266 *vs* 799 ± 266; $P = 0.05$). The circulating levels of IL-6 were significantly higher in tobacco-exposed sham compared to tobacco-naïve sham rats ($28\,177 \pm 2415$ *vs* 464 ± 83; $P = 0.001$) and in tobacco-exposed MI compared to tobacco-naïve MI rats ($29\,192 \pm 3273$ *vs* $13\,082 \pm 1664$; $P = 0.001$) and IFN-γ levels were also significantly higher in tobacco-exposed sham compared to tobacco-naïve sham (4023 ± 616 *vs* 2438 ± 343; $P = 0.05$) and in tobacco-exposed MI compared to tobacco-naïve MI rats (7753 ± 626 *vs* 3634 ± 379; $P = 0.01$). Similarly, the levels of TNF-α were significantly higher in tobacco-exposed sham compared to tobacco-Naïve sham (1600 ± 214 *vs* 379 ± 83; $P = 0.05$) and in tobacco-exposed MI compared to tobacco-naïve MI rats (2494 ± 143 *vs* 888 ± 234; $P = 0.001$). The serum levels in NAC-treated rats compared

Table 2 Sequential changes of fractional shortening in different groups studied[a]

Condition	Week 1	Week 2	Week 3	Week 4	Week 5	Week 6
Tobacco-naïve sham	55.5 ± 3.4[b]	56.5 ± 2.8	55 ± 2.9	58.1 ± 4.2	57.1 ± 2.9	55.1 ± 3.5
Tobacco-exposed sham	51.3 ± 2.4	49.1 ± 2.7	45.3 ± 3.4	41.2 ± 2.6	37 ± 2.8	35.1 ± 1.3
Tobacco-naïve MI	34.3 ± 2.1	33.5 ± 1.5	31.1 ± 3.3	30.8 ± 0.8	28.4 ± 1.1	27.4 ± 2.3
Tobacco-exposed MI	26.3 ± 3.2	24.6 ± 3.5	22.8 ± 2.6	20.6 ± 2.8	19.3 ± 1.6	16.4 ± 0.2
Tobacco-naïve MI+NAC	37.2 ± 1.9	ND	ND	ND	ND	45.7 ± 2.1
Tobacco exposed MI+NAC	26.3 ± 0.7	28.4 ± 0.6	31.7 ± 1.8	34.2 ± 1.1	36.1 ± 1.5	37.6 ± 0.56

ND, not determined.

[a]Percent fractional shortening analysis for rats with and without exposure to cigarette smoke, myocardial infarction and treatment with *N*-acetyl cysteine ranging from weeks 1 to 6 are shown; the results are presented as mean ± s.e.m.

[b]Percent fractional shortening.

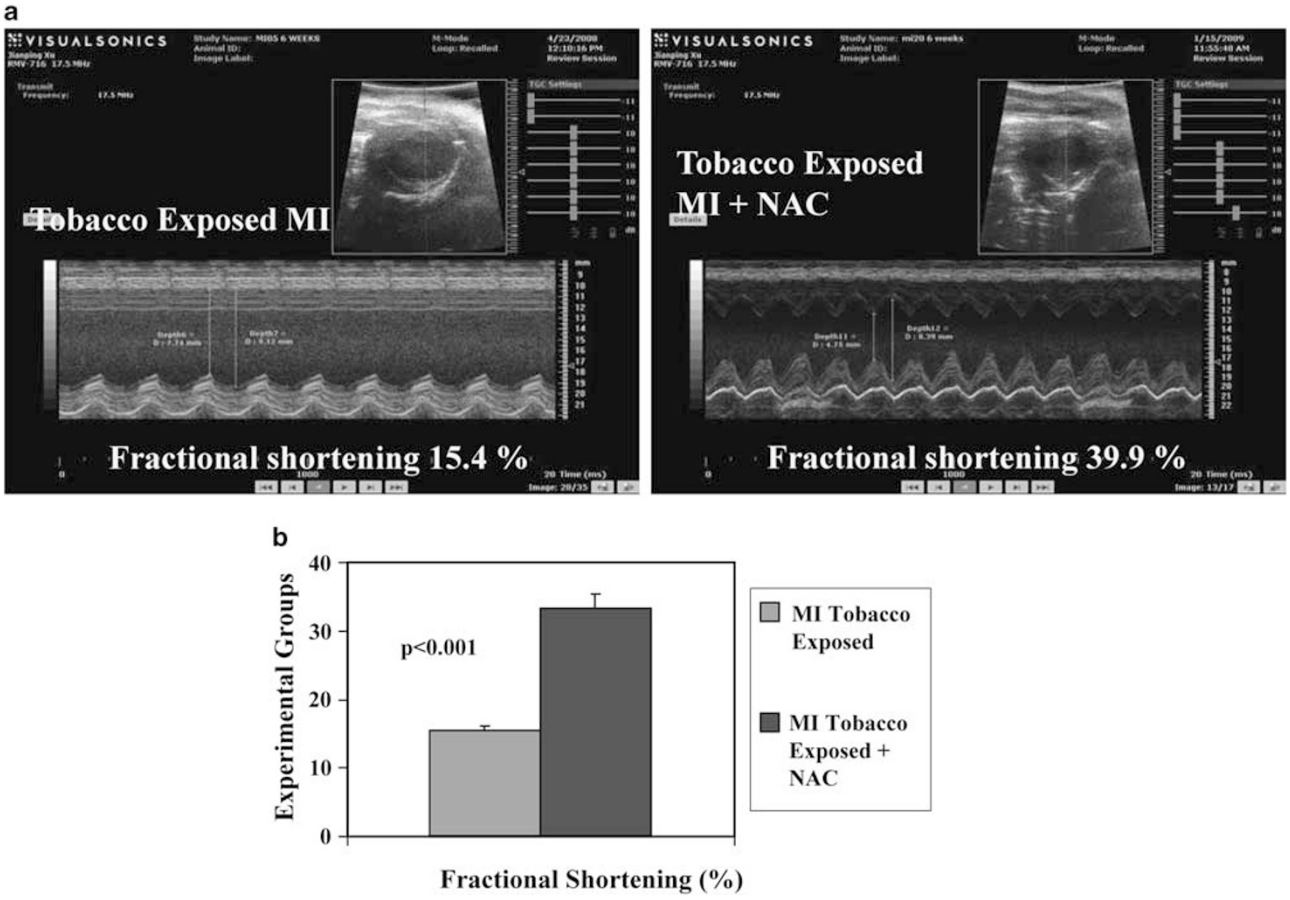

Figure 4 (**a**) Comparison of echocardiography analysis of tobacco-exposed myocardial infarction (MI) rats with and without *N*-acetyl cysteine: typical M-mode images of parasternal short-axis view at the middle of the papillary muscle level, which are shown for representative tobacco-exposed MI rat without and with *N*-acetyl cysteine. Individual fractional shortening (%) for each rat is shown. (**b**) Mean ± s.e.m. of fraction shortening (%) for tobacco-exposed MI rats and tobacco-exposed MI rats with *N*-acetyl cysteine is also shown.

to tobacco-exposed MI decreased significantly for IL-1α (1271 ± 143 *vs* 369 ± 72; $P = 0.0005$), IL-1β (3014 ± 326 *vs* 676 ± 56; $P = 0.0001$), IL-2 (1766 ± 266 *vs* 1380 ± 224; $P = 0.01$), IL-6 (29 192 ± 3273 *vs* 10 515 ± 1241; $P = 0.0006$), IFN-γ (7753 ± 626 *vs* 1334 ± 60; $P = 0.00001$) and TNF-α (2494 ± 182 *vs* 511 ± 120; $P = 0.001$).

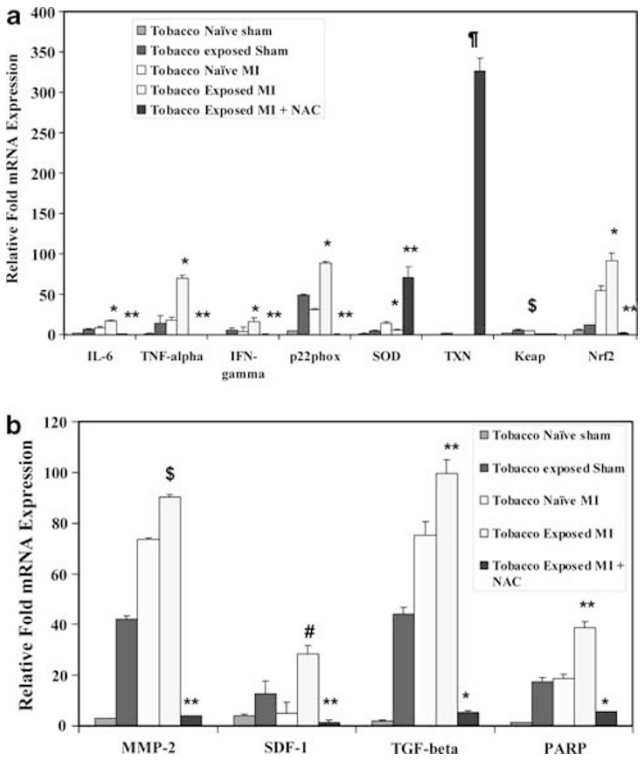

Figure 5 Effect of *N*-acetyl cysteine on tobacco-induced intracardiac mRNA expression. (**a**) *Pro-inflammatory cytokines*: the mRNA expression of interleukin (IL)-6, tumor necrosis factor (TNF)-α and interferon (IFN)-γ in cardiac tissues from tobacco-naïve sham ($n=3$), tobacco-exposed sham ($n=3$), tobacco-naïve myocardial infarction (MI) ($n=3$) and tobacco-exposed MI rats ($n=4$) was studied by real-time polymerase chain reaction (PCR). The results are presented as normalized fold expression (mean ± s.e.m., $n=3$) using β-*actin* as a reference gene. $^{*}P=0.001$ for TNF-α, IL-6 and IFN-γ mRNA (tobacco-naïve *vs* tobacco-exposed rats with MI); $^{**}P=0.001$ for TNF-α, IL-6 and IFN-γ mRNA (tobacco-exposed MI *vs* and tobacco-exposed MI rats *vs N*-acetyl cysteine-treated tobacco-exposed MI rats). *Oxidative stress molecules*: $^{*}P=0.001$, increased $p22^{phox}$ and decreased superoxide dismutase (SOD) mRNA; $^{**}P<0.001$, decreased thioredoxin (TXN) mRNA (tobacco-naïve *vs* and tobacco-exposed rats with MI); $^{*}P=0.001$, increased SOD mRNA, $^{¶}P=0.0001$, increased TXN mRNA (tobacco-exposed MI *vs* and tobacco-exposed MI rats *vs N*-acetyl cysteine-treated tobacco-exposed MI rats), $p22^{phox}$ mRNA was not detectable. $^{\$}P=0.05$ for Kelch ECH-associating protein 1 (Keap-1) mRNA (tobacco-naïve *vs* and tobacco-exposed rats with MI); $^{**}P=0.001$ for nuclear factor-E2-related factor 2 (Nrf2) mRNA (tobacco-naïve *vs* and tobacco-exposed rats with MI); $^{**}P=0.001$ for Nrf2-2 and Keap-1 mRNA (tobacco-exposed MI *vs* and tobacco-exposed MI rats *vs N*-acetyl cysteine-treated tobacco-exposed MI rats). (**b**) *Tissue repair molecules*: $^{\$}P=0.05$ for MMP-2 mRNA (tobacco-naïve *vs* tobacco-exposed rats with MI); $^{\#}P=0.01$ for stromal-derived factor-1 (SDF-1) mRNA (tobacco-naïve *vs* and tobacco-exposed rats with MI); $^{**}P=0.001$ for MMP-2 and SDF-1 mRNA (tobacco-exposed MI *vs* tobacco-exposed MI rats *vs N*-acetyl cysteine-treated tobacco-exposed MI rats); $^{*}P=0.001$, increased tumor growth factor (TGF)-β and poly-(ADP-ribose) polymerase (PARP) mRNA (tobacco-naïve *vs* tobacco-exposed MI rats); $^{**}P=0.001$, decreased TGF-β and PARP mRNA (tobacco-exposed MI *vs* and tobacco-exposed MI rats *vs N*-acetyl cysteine-treated tobacco-exposed MI rats).

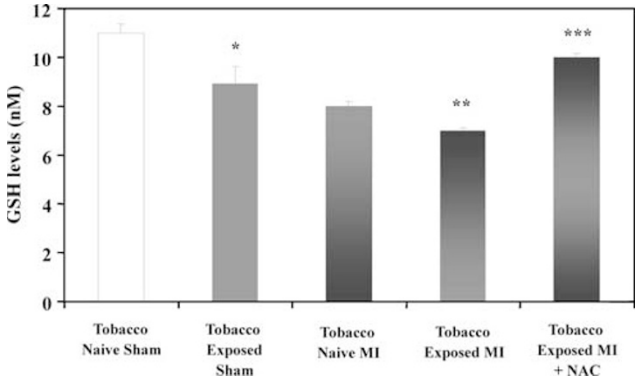

Figure 6 Effect of *N*-acetyl cysteine on glutathione levels. We quantified serum levels of glutathione using a luciferase activity based kit from Promega in serum samples from tobacco-exposed sham, tobacco-naïve sham, tobacco-exposed myocardial infarction (MI) rats and tobacco-naïve MI rats. $^{*}P=0.04$, tobacco exposed sham *vs* tobacco-naïve sham; $^{**}P=0.009$, tobacco-exposed MI *vs* tobacco-naïve MI; $^{***}P\leqslant 0.001$, tobacco-exposed MI *vs* tobacco-exposed MI + *N*-acetyl cysteine.

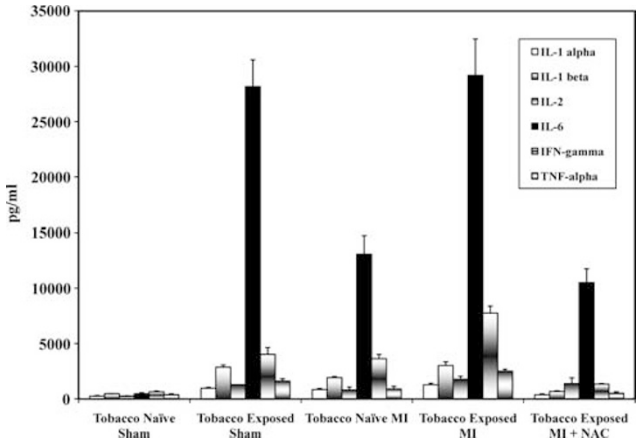

Figure 7 Effect of *N*-acetyl cysteine on tobacco-induced circulating levels of pro-inflammatory cytokines. We quantified circulating levels of pro-inflammatory cytokines using a BioPlex rat cytokine assay kit (Bio-Rad) in the serum obtained from tobacco-exposed sham, tobacco-naïve sham, tobacco-exposed myocardial infarction (MI) and tobacco-naïve MI rats. The results are expressed as mean ± s.e.m. (pg/ml). A significant decreased circulating level of cytokines in *N*-acetyl cysteine-treated rats is shown.

DISCUSSION

Our results are supportive of the concept that chronic exposure to tobacco results in the depression of cardiac function, which worsens even further in the setting of an acute MI. These sentinel findings confirm the damaging effect of chronic tobacco exposure in determining post-infarction ventricular remodeling. The model used in our investigation was distinctive. We first exposed rats to conditions that simulate the condition of chronic habitual smoking. The validity of this model has been published previously.[1] We then investigated the outcomes of these rats with respect to ventricular function and structural damage in the setting an acute MI and with abrupt cessation of smoking exposure (as is typically noted in the human condition). Thereafter, we tested whether the extent of damage could be ameliorated by using an easily available therapy in the form

of dietary supplement NAC, which specifically targeted those molecular pathways that are aberrant in the setting of tobacco-related damage. We find that NAC can not only abrogate the inflammatory and pro-oxidant pathways upregulated in this model, but also results in improved ventricular remodeling, reduced myocardial damage, and thus facilitates myocardial repair in acute MI.

Previous studies, using an acute cigarette inhalation model, have demonstrated changes in diastolic function.[34–36] We extend these findings in a model of chronic tobacco exposure, which indicate the presence of systolic function impairment and that arbiters of this response include molecular pathways of increased inflammation and oxidative stress. It is known that there is no detectable mRNA expression of pro-inflammatory cytokines in normal myocardial tissue,[37] but once cardiac injury sets in (such as with an MI), the intracardiac expression of IL-6, TNF-α and IFN-γ mRNA expression possibly mediate the events of remodeling in the myocardium as reported earlier.[38–42] An increased expression of these cytokines may result in enhanced production of tissue repair molecules. Our results support this assumption, as myocardial mRNA expression of MMP-2, SDF-1 and TGF-β was significantly higher in chronic tobacco-exposed rats compared with tobacco-naïve rats with MI. It is likely that the increased expression of these molecules in tobacco-exposed rats not only signifies their role in altered remodeling in the myocardium, but also the direct effect of tobacco exposure on the expression of these tissue repair participants. Similarly, tobacco exposure also resulted in a significantly higher mRNA expression of PARP, a marker of DNA damage and indicator of apoptosis,[43,44] suggesting that the more extensive MI in tobacco-exposed rats is also accompanied by an increase in cardiomyocyte apoptosis.

We also show a marked increase in oxidative stress in rats with MI previously exposed to chronic tobacco smoke compared to tobacco-naïve rats. This was demonstrated by increased expression of the NADPH oxidase component $p22^{phox}$. The integral membrane protein $p22^{phox}$ is an indispensable component of the superoxide-generating phagocyte NADPH oxidase, which is a central molecule in the production of superoxides.[45–49] Conversely, the expression of antioxidants SOD and TXN decreased significantly in infarcted myocardium of rats exposed to tobacco smoke compared to tobacco naïve.

We also explored the expression of the Keap 1-Nrf2–antioxidant response element signaling pathway that is known to regulate several protective mechanisms, including the expression of antioxidant and anti-inflammatory events.[50–52] It is also known that the adaptive response induced by 4-hydroxynonenal, one of the important determinants of oxidative stress, is positively mediated by gene expression of cyto-protective protein (Nrf2/Keap-1) pathway.[53] Our results suggest the critical role of Nrf2/Keap1 pathway in the stimulation of oxidative stress by chronic tobacco exposure because cigarette smoke exposure resulted in the activation of Nrf2 mRNA expression that counteract the immense oxidative stress that accompanies this trigger. These results are supported by a recent study,[54] which demonstrated that Nrf2 is activated in the small airway epithelium of healthy smokers. Other *in vitro* studies on different cells types have also suggested the increased Nrf2 expression in response to cigarette smoke extracts,[55] indicating the protective role of Nrf2 in cigarette smoke-induced health disorders. A significant inhibition of Nrf2 mRNA expression in NAC-treated rats supports this assumption, as in the absence of oxidative stress, Nrf2 expression was not activated. Alternatively, in the presence of cigarette smoke, Nrf2 may stay in the cytoplasm, and in the presence of NAC, it travels to the nucleus and ensue the transcription of antioxidants and inhibits inflammation.

The positive effects of the treatment with NAC that reverses the sequel of acute MI suggest that it targets both vascular inflammation and oxidative stress leading to the consequent facilitation of tissue repair. Although our intent was to see if NAC could counter the deleterious effects of inflammatory and oxidative stress pathways in chronic tobacco-exposed situations, we cannot ignore the fact that this may be an equally viable strategy for non-smokers with MI.

One of the weaknesses of this study is that the gene and protein expression reported are based on a single time point of 6 weeks; however, a time course of the effect of NAC on cardiac function could provide better results with regard to the efficacy of NAC on MI. Also, these results are obtained during continued smoking till 6 weeks; the studies in animals post-cessation of smoking may also provide interesting data on the effect of smoking on cardiac dysfunction. The numbers for each group are between 3 and 5 due to very laborious effort during exposure to cigarette smoke as well as the analysis of cardiac dysfunction using echocardiography each week for all the animals.

In conclusion, we demonstrate the efficacy of antioxidant glutathione precursor NAC to limit the extent of MI and facilitate tissue repair and preservation of ventricular function in the setting of chronic tobacco exposure. Such a simple therapy was based on a dietary supplement.

ACKNOWLEDGEMENTS

This work was supported by a Grant from the University of Maryland Statewide Health Network and other Tobacco-Related Diseases Research Grant through the Maryland Cigarette Restitution Fund Program.

DISCLOSURE/CONFLICT OF INTEREST

The authors declare no conflict of interest.

1. Khanna A, Xu J, Uber P, *et al.* Pre-transplant donor or recipient tobacco smoke exposure accelerates cardiac allograft rejection, vasculopathy and graft loss. Circulation 2009;120:1814–1821.
2. Tomaki M, Sugiura H, Koarai A, *et al.* Decreased expression of antioxidant enzymes and increased expression of chemokines in COPD lung. Pulm Pharmacol Ther 2007;20:596–605.
3. Mendall MA, Patel P, Ballam L, *et al.* C reactive protein and its relation to cardiovascular risk factors: a population based cross sectional study. BMJ 1996;312:1061–1065.

4. Tracy RP, Psaty BM, Macy E, *et al.* Lifetime smoking exposure affects the association of C-reactive protein with cardiovascular disease risk factors and subclinical disease in healthy elderly subjects. Arterioscler Thromb Vasc Biol 1997;17:2167–2176.
5. Hasday JD, Bascom R, Costa JJ, *et al.* Bacterial endotoxin is an active component of cigarette smoke. Chest 1999;115:829–835.
6. Churg A, Wang RD, Tai H, *et al.* Macrophage metalloelastase mediates acute cigarette smoke-induced inflammation via tumor necrosis factor-alpha release. Am J Respir Crit Care Med 2003;167:1083–1089.
7. Foronjy RFO, Propokenko O, Lemaitre V, *et al.* Superoxide dismutase expression attenuates cigarette smoke- or elastase-generated emphysema in mice. Am J Resp Crit Care Med 2006;173:623–631.
8. Kato T, Inoue T, Morooka T, *et al.* Short-term passive smoking causes endothelial dysfunction via oxidative stress in nonsmokers. Can J Physiol Pharmacol 2006;84:523–529.
9. Aycicek A, Erel O, Kocyigit A. Decreased total antioxidant capacity and increased oxidative stress in passive smoker infants and their mothers. Pediatr Int 2005;47:635–639.
10. Iizuka T, Ishii Y, Itoh K, *et al.* Nrf2-deficient mice are highly susceptible to cigarette smoke-induced emphysema. Genes Cells 2005;10:1113–1125.
11. Sobczak A, Golka D, Szoltysek-Boldys I. The effects of tobacco smoke on plasma alpha- and gamma-tocopherol levels in passive and active cigarette smokers. Toxicol Lett 2004;151:429–437.
12. Harman SM, Liang L, Tsitouras PD, *et al.* Urinary excretion of three nucleic acid oxidation adducts and isoprostane F(2)alpha measured by liquid chromatography-mass spectrometry in smokers, ex-smokers, and nonsmokers. Free Radic Biol Med 2003;15:1301–1309.
13. Koul A, Singh A, Sandhir R. Effect of alpha-tocopherol on the cardiac antioxidant defense system and atherogenic lipids in cigarette smoke-inhaling mice. Inhal Toxicol 2003;15:513–522.
14. Wang S, Sun NN, Zhang J, *et al.* Immunomodulatory effects of high-dose alpha-tocopherol acetate on mice subjected to sidestream cigarette smoke. Toxicology 2002;175:235–245.
15. Szocs K, Lassègue B, Sorescu D, *et al.* Upregulation of Nox-based NAD(P)H oxidases in restenosis after carotid injury. Arterioscler Thromb Vasc Biol 2002;22:21–22.
16. Penna C, Mancardi D, Rastaldo R, *et al.* Cardioprotection: a radical view free radicals in pre and postconditioning. Biochim Biophys Acta 2009;1787:781–793.
17. Looi YH, Grieve DJ, Siva A, *et al.* Involvement of Nox2 NADPH oxidase in adverse cardiac remodeling after myocardial infarction. Hypertension 2008;51:319–325.
18. Sirker A, Zhang M, Murdoch C, *et al.* Involvement of NADPH oxidases in cardiac remodelling and heart failure. Am J Nephrol 2007;27:649–660.
19. Zhao L, Roche BM, Wessale JL, *et al.* Chronic xanthine oxidase inhibition following myocardial infarction in rabbits: effects of early versus delayed treatment. Life Sci 2008;82:495–502.
20. Doerries CK, Hilfiker-Kleiner D, Luchtefeld M, *et al.* Critical role of the NAD(P)H oxidase subunit p47phox for left ventricular remodeling/dysfunction and survival after myocardial infarction. Circ Res 2007;100:894–903.
21. Qin F, Simeone M, Patel R. Inhibition of NADPH oxidase reduces myocardial oxidative stress and apoptosis and improves cardiac function in heart failure after myocardial infarction. Free Radic Biol Med 2007;43:271–281.
22. Chen Z, Siu B, Ho YS, *et al.* Overexpression of MnSOD protects against myocardial ischemia/reperfusion injury in transgenic mice. J Mol Cell Cardiol 1998;30:2281–2289.
23. Wang P, Chen H, Qin H, *et al.* Overexpression of human copper, zinc-superoxide dismutase (SOD1) prevents postischemic injury. Proc Natl Acad Sci USA 1998;95:4556–4560.
24. Date MO, Morita T, Yamashita N, *et al.* The antioxidant *N*-2-mercaptopropionyl glycine attenuates left ventricular hypertrophy in *in vivo* murine pressure-overload model. J Am Coll Cardiol 2002;39:907–912.
25. Tsujimoto I, Hikoso S, Yamaguchi O, *et al.* The antioxidant edaravone attenuates pressure overload-induced left ventricular hypertrophy. Hypertension 2005;45:921–926.
26. Oskarsson HJ, Coppey L, Weiss RM, *et al.* Antioxidants attenuate myocyte apoptosis in the remote non-infarcted myocardium following large myocardial infarction. Cardiovasc Res 2000;45:679–687.
27. Sia YT, Parker TG, Liu P, *et al.* Improved post-myocardial infarction survival with probucol in rats: effects on left ventricular function, morphology, cardiac oxidative stress and cytokine expression. J Am Coll Cardiol 2002;39:148–156.
28. Siveski-Iliskovic N, Kaul N, Singal PK. Probucol promotes endogenous antioxidants and provides protection against adriamycin-induced cardiomyopathy in rats. Circulation 1994;89:2829–2835.
29. Nakamura R, Egashira K, Machida Y, *et al.* Probucol attenuates left ventricular dysfunction and remodeling in tachycardia-induced heart failure: roles of oxidative stress and inflammation. Circulation 2002;106:362–367.
30. Betge S, Lutz K, Roskos M, *et al.* Oral treatment with probucol in a pharmacological dose has no beneficial effects on mortality in chronic ischemic heart failure after large myocardial infarction in rats. Eur J Pharmacol 2007;558:119–127.
31. Hoshida S, Yamashita N, Igarashi J, *et al.* Long-term probucol treatment reverses the severity of myocardial injury in watanabe heritable hyperlipidemic rabbits. Arterioscler Thromb Vasc Biol 1997;17:2801–2807.
32. Xu L, Cai BQ, Zhu YJ. Pathogenesis of cigarette smoke-induced chronic obstructive pulmonary disease and therapeutic effects of glucocorticoids and *N*-acetylcysteine in rats. Chin Med J (Engl) 2004;117:1611–1619.
33. Xu J, Zhang C, Khanna A. Wideband high frequency echocardiography to evaluate myocardial infarct size. J Ultrasound Med 2009;28:1501–1509.
34. Gu L, Pandey V, Geenen DL, *et al.* Cigarette smoke-induced left ventricular remodelling is associated with activation of mitogen-activated protein kinases. Eur J Heart Fail 2008;10:1057–1064.
35. Castardeli E, Duarte DR, Minicucci MF, *et al.* Tobacco smoke-induces left ventricular remodeling is not associated with metalloproteinase-2 or -9 activation. Eur J Heart Fail 2007;9:1081–1085.
36. Castardeli E, Paiva SA, Matsubara BB, *et al.* Chronic cigarette smoke exposure results in cardiac remodeling and impaired ventricular function in rats. Arq Bras Cardiol 2005;84:320–324.
37. Chandrasekar B, Colston JT, Freeman GL. Induction of proinflammatory cytokine and antioxidant enzyme gene expression following brief myocardial ischaemia. Clin Exp Immunol 1997;108:346–351.
38. Debrunner M, Schuiki E, Minder E, *et al.* Proinflammatory cytokines in acute myocardial infarction with and without cardiogenic shock. Clin Res Cardiol 2008;97:298–305.
39. Samnegård A, Hulthe J, Silveira A, *et al.* Gender specific associations between matrix metalloproteinases and inflammatory markers in post myocardial infarction patients. Atherosclerosis 2009;202:550–556.
40. Kelishadi R, Sabri M, Motamedi N, *et al.* Factor analysis of markers of inflammation and oxidation and echocardiographic findings in children with a positive family history of premature coronary heart disease. Pediatr Cardiol 2009;30:477–481.
41. Orn S, Manhenke C, Ueland T, *et al.* C-reactive protein, infarct size, microvascular obstruction, and left-ventricular remodelling following acute myocardial infarction. Eur Heart J 2009;30:1180–1186.
42. Schulz R, Heusch G. Tumor necrosis factor-alpha and its receptors 1 and 2: Yin and Yang in myocardial infarction? Circulation 2009;119:1355–1357.
43. Zingarelli B, Hake PW, O'Connor M, *et al.* Differential regulation of activator protein-1 and heat shock factor-1 in myocardial ischemia and reperfusion injury: role of poly(ADP-ribose) polymerase-1. Am J Physiol Heart Circ Physiol 2004;286:H1408–H1415.
44. Palfi A, Toth A, Hanto K, *et al.* PARP inhibition prevents postinfarction myocardial remodeling and heart failure via the protein kinase C/glycogen synthase kinase-3beta pathway. J Mol Cell Cardiol 2006;41:149–159.
45. Zalba G, San José G, Moreno MU, *et al.* NADPH oxidase-mediated oxidative stress: genetic studies of the p22 (phox) gene in hypertension. Antioxid Redox Signal 2005;7:1327–1336.
46. Kou B, Zhang J, Singer DR. Effects of cyclic strain on endothelial cell apoptosis and tubulogenesis are dependent on ROS production via NAD(P)H subunit p22phox. Microvasc Res 2009;77:125–133.
47. Manea A, Manea SA, Gafencu AV, *et al.* AP-1-dependent transcriptional regulation of NADPH oxidase in human aortic smooth muscle cells: role of p22phox subunit. Arterioscler Thromb Vasc Biol 2008;28:878–885.
48. Kawahara T, Ritsick D, Cheng G, *et al.* Point mutations in the proline-rich region of p22phox are dominant inhibitors of Nox1- and

Nox2-dependent reactive oxygen generation. J Biol Chem 2005; 280:31859–31869.
49. Modlinger P, Chabrashvili T, Gill PS, *et al.* RNA silencing *in vivo* reveals role of $p22^{phox}$ in rat angiotensin slow pressor response. Hypertension 2006;47:238–244.
50. Zhang DD. Mechanistic studies of the Nrf2-Keap1 signaling pathway. Drug Metab Rev 2006;38:769–789.
51. Nguyen T, Nioi P, Pickett CB. The Nrf2-ARE signaling pathway and its activation by oxidative stress. J Biol Chem 2009;284:13291–13295.
52. Mann GE, Bonacasa B, Ishii T, *et al.* Targeting the redox sensitive Nrf2-Keap1 defense pathway in cardiovascular disease: protection afforded by dietary isoflavones. Curr Opin Pharmacol 2009;9:139–145.
53. Levonen AL, Landar A, Ramachandran A, *et al.* Cellular mechanisms of redox cell signalling: role of cysteine modification in controlling antioxidant defenses in response to electrophilic lipid oxidation products. Biochem J 2004;378:373–382.
54. Hübner RH, Schwartz JD, De Bishnu P, *et al.* Coordinate control of expression of Nrf2-modulated genes in the human small airway epithelium is highly responsive to cigarette smoking. Mol Med 2009;15:203–219.
55. Knörr-Wittmann C, Hengstermann A, Gebel S, *et al.* Characterization of Nrf2 activation and heme oxygenase-1 expression in NIH3T3 cells exposed to aqueous extracts of cigarette smoke. Free Radic Biol Med 2005;39:1438–1448.